Failure Impact Energy in Curved Composite Plates

Nawres J. Nasser
Mechanical Department, Institute of Technology-Baghdad, Foundation of Technical Education
nawresjabaar@yahoo.com

Dr. Sajeda K. Radi
MechanicalEngineeringDepartment, Collage of Engineering, Al-Mustansiriya University
sajeda10122008@yahoo.com

Dr. Khaldoon A. Al-Jubouri
MechanicalEngineeringDepartment, Collage of Engineering, Al-Mustansiriya University
dr.khaldoon2010@yahoo.com

Abstract

An investigation of low velocity impact characteristics of curved composite plates have been presented. The plates represent parts of car's bumpers with radii of curvature of 120mm, 200mm, 300mm, 450mm and infinity.
Two types of composite materials are used, unidirectional 0° and woven 0°/90° types with five layers of 3mm thickness and ten layers of 6mm thickness of each type.
The results showed that larger plates curvatures can absorb more impact energy and the ten layer woven 0°/90° composite are superior to similar unidirectional 0° composite. On the other hand the five layer unidirectional 0° plates are superior in absorbing energy compared to similar woven 0°/90° plates.
An investigation of the failure patterns and development for both types of composite has been presented and discussed.
The effects of multi-strike on the energy absorbtion of both type of composite have showed different pattern of energy absorbtion behavior.

Key words: ***Impact, Curved plate, Composite, Failure energy***

الخلاصة

يتضمن البحث دراسة خواص الصدم للسرع الواطئة للألواح المقوسة المصنوعة من مواد مركبة. الألواح تمثل أجزاء من مصدات السيارات وبأنصاف أقطار تقوس 120 ملم، 200 ملم، 300 ملم، 450 ملم وألواح مستوية. تم اختيار نوعين من المواد المركبة هي ذات الألياف الزجاجية أحادية الاتجاه وذات الألياف الزجاجية المحاكة بصورة متعامدة. لكلا النوعين تم اختبار ألواح ذات خمس طبقات بسمك 3 ملم وألواح ذات عشر طبقات بسمك 6 ملم.
النتائج أظهرت أن الألواح المركبة ذات التقوسات الأكبر (أي أنصاف الأقطار الأصغر) لها القابلية على امتصاص مقادير اكبر من الطاقة وان الألواح من ألياف الزجاج المحاكة بصورة متعامدة وبعشر طبقات قد تفوقت على الألواح المماثلة من الألياف المتوازية (ذات الاتجاه الواحد)، بينما تفوقت الألواح ذات خمس طبقات من الألياف المتوازية على مثيلتها من الألواح ذات الألياف المحاكة بصورة متعامدة.
يقدم البحث كذلك دراسة لنمط الفشل وتطوره في كلا النوعين من الألواح المفحوصة.

تمت دراسة تأثير ضربات الصدم المتلاحقة على قابلية الألواح المركبة في امتصاص الطاقة ووجد أن سلوكها في هذا المجال يختلف حسب نوع واتجاه الألياف المستخدمة في صنعها.

1-Introduction

The idea of composite materials itself is not new. Composite materials have a long history of usage buttheir beginning is unknown. However, all recorded history contains references to some forms of composite materials[**1**]. The numerous advantages of fibre-reinforced composites, including their high specific mechanical properties, have led to their increasing use in many fields of engineering. It has long been recognised that these materials are sensitive to impact damage, especially out-of-plane impact, which can induce damage even at very low impact energies[**2**].

Due to the anisotropy of composite laminates and non-uniform distribution of stress under dynamic loading, the failure process of laminates is very complex[**3**]. This sensitivity to impact damage is due in part to the brittle behavior of the fibres used to reinforce such composites, and even of the resins used for the matrix phase. Hence, there has been a lot of work carried out in the field of composites impact, mostly for expensive, high- Vf carbon/epoxy laminates used mainly in the aerospace industry. Ball and bar impactors are used to study both static and low-velocity impact response of graphite/epoxy , finding that the impact damage varied not only with incident energy, but also with incident velocity.

The aim of this study is to investigate the effect of curvature of bumpers on energy absorbtion due to impact. Unidirectional and woven E-glass at two thicknesses 3 and 6 mm are to be investigated. The behavior of cracks in the utilized composite material are also studied.

2- Literature Review

The study of impact behavior of composite received much attention in the last 20 years or so. Henkhaus[**4**] presented a comprehensive overview of research involving the general behavior of composite structures subjected to impact loading.

The recent progress in materials modeling and numerical simulation of the impact response of fiber-reinforced composite structures is reported by Johnsona et al[**5**].

An imported study based on experimental tests of the damage characteristics and failure strength of different composite laminates is presented by Shyr and Pan[**6**]. In this report, the failure development in tested specimens was well identified and fully described for each type of composite material.

Reports on experimental investigation of impact on composite plates include Sutherland and Soures[**7**][**2**] work on low-energy drop weight impact test on woven and E-glass/polyester composite. Hosseinzadeh et al[**8**] studied the damage zones of four different types of fiber reinforced plates.

Theoretical studies in this field included Tita et al[9] work on the stacking sequence influence on impact energy using a finite element analysis. Davies and Zhang [10] presented a model for the strategy of predicting internal damage in composite structures. Another study by Her and Liang [11] used ANSYS/LS-DYNA software to study low velocity impact on composite plates and shell. Another finite element analysis is presented by Rao[12] for a doubly curved quadrilateral shell. Other numerical studies include Khalili et al[13] work using ABAQUS code, Krishnamurthy et al[14] study of impact response of composite shells. The later used both Fourier series and the finite element methods in their analysis.

All of the above reported literature dealt with flat composite plates. Very few reports are available in the literature dealing with impact on curved composite plates. An important report in this field is that of Kim et al[15]. The dynamic behavior and impact damage of curved plates is analysed and a finite element model is developed for some types of structures. Another theoretical study in this field is reported by Kumar[16] dealing with impact-induced damage in curved composite laminates.

3-Experimental Work

3-1 Experimental Test Rig

Despite the importance of impact testing of composite materials in mechanical engineering applications, suitable devices are not available in any local university. As this research deals with the impact behavior of composite materials ,it was decided to build an experimental rig to perform standard tests in this field.

The design, construction and testing of the rig is the subject of a separate report to be published later and the experimenting rig and set up are shown in figure(1). This rig was bult in Mechanical Engineering Department College of Engineering Al-Mustansiriya University.

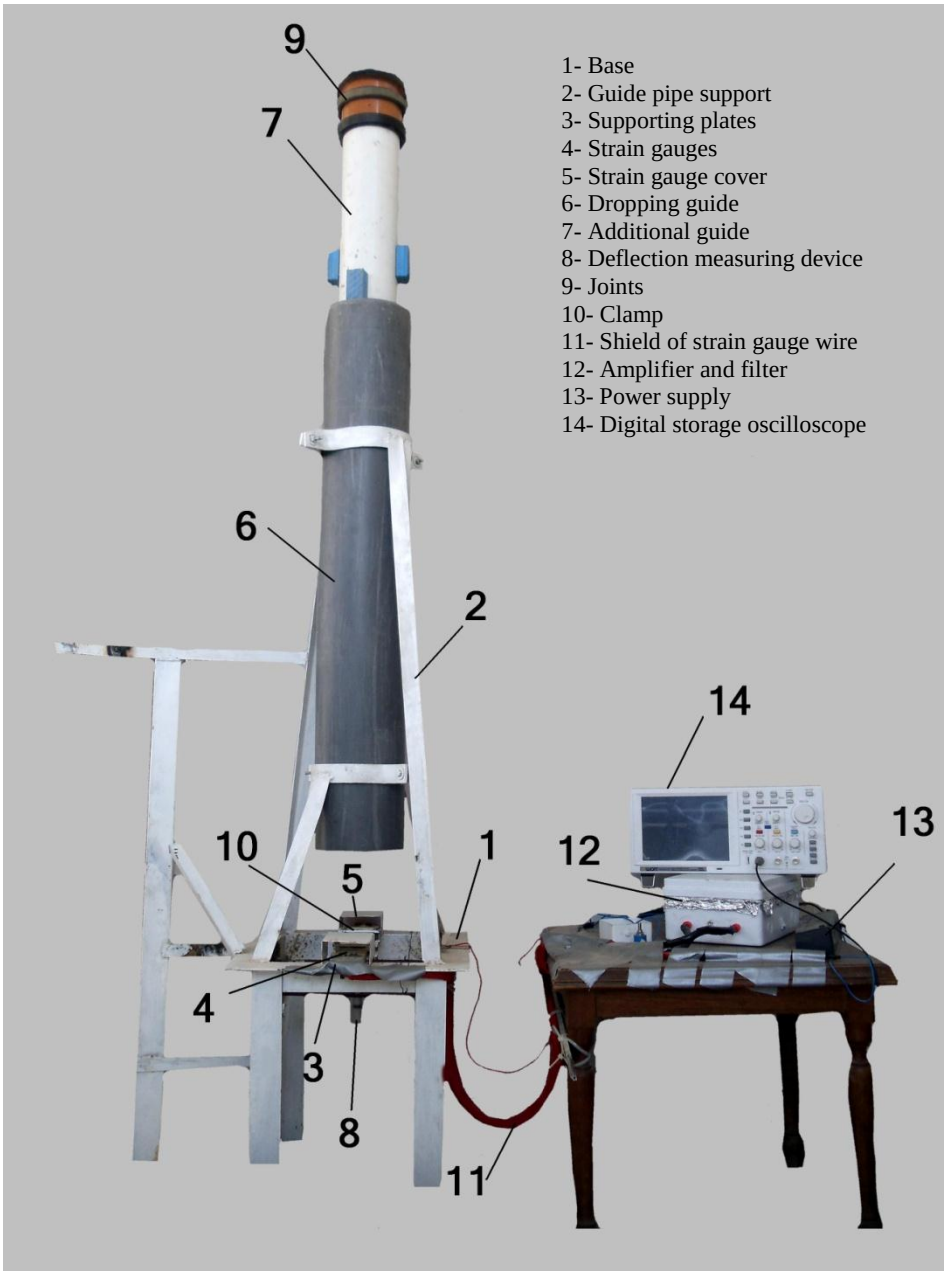

Figure (1) Impact test rig

The rig consist essentially of a group of pipes to function as a variable height guide for the impactor. A steel ball of 100mm diameter weighing 2.8 kg is used as the impactor.

The base of the rig is equipped with two stainless steel, strain gauged plates fixed with one end at opposite sides of the base. Composite plates can be clamped in-between these two strain gauged plates.

3-2 Specimens

The basic constituents of the composite materials used in this work are reinforcing woven fibers, reinforcing roving fibers and the matrix resin. The mechanical properties of polyester resins are shown in table (1).The specifications of the E-glass fibers are shown in table (2).

Table (1) The set of typical properties for polyester resins [17]

Property	Polyesters resins
Density	1,200 kg/m3
Tensile modulus	2.8–3.5 GPa
Tensile fracture stress	50–80 MPa
Compressive fracture stress	90–200 MPa
Shear fracture stress	10–20 MPa

Table (2) Mechanical properties of E-glass fibers [18]

Properties	Value
Density	2540 kg/m^3
Tensile Strength	3.45 GPa
Modulus of Elasticity	72.4 GPa
Yield Elongation	4.8%
Poisson's ratio	0.22

The tests specimens different curvature radii are shown in figure (2)

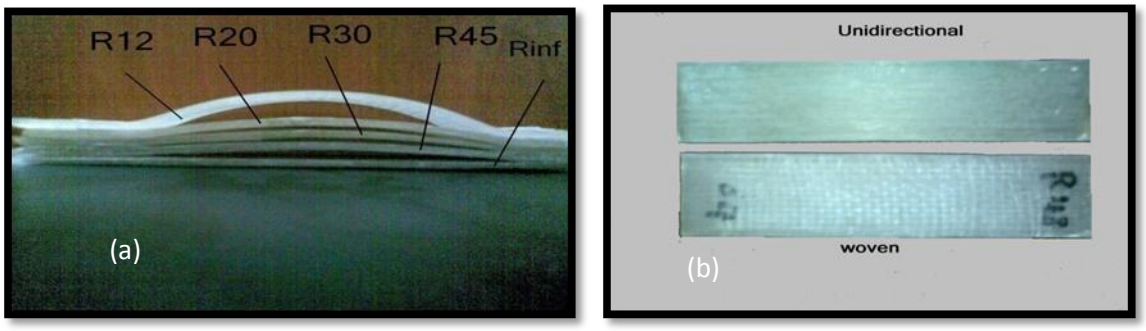

Figure (2) a- Radii of all specimens
b- Top view of woven and unidirectional specimen after cleaning

Five moulds were needed for the manufacture of the specimens. A wood panels was used with dimensions (10*6.25 cm) with a length of (105 cm). The whole wood panel sides were smoothed using a phasing machine. The panel was then cut into five equal pieces of (20 cm)in length. Each of the pieces was cut in to two (4.5*5 cm) parts forming the upper and lower parts of the molds. The upper part was shaved to the required curvature while the lower part was glued to an additional piece of wood of (5*1.7 cm) and (12 cm) in length. This piece was then shaved to form the required curvature for each mold. Using this process, five complete molds of radius (R_1=120, R_2=200, R_3=300, R_4=450, R_5=∞ mm) were produced.

pieces of smooth wood with dimension of (96*17 mm) having the same length of (20 cm) as that of the mold were glued to both sides of the lower part of each mold. These five molds are shown in figure (3). All together (130) specimens were made with a volume fraction of 33%.

Figure (3) The five molds

3-3 Experimental procedure

This procedure involved, connecting the strain gauge circuit with amplifier is connected to the Digital Storage Oscilloscope which is in turn is connected with a computer to save the signal output. The specimen is then fixed to the strain gauged frame.

The specimen is subjected to consecutive strikes with increasing heights until failure. This gave an indication of the required drop height causing failure. A new specimen is then fixed and struck at a height larger than that causing cumulative failure. The process is continued by changing samples and increase the height until specimen failure. By this process the height required to fail the specimen with one strike is identified. At the same time and after each strike the maximum deflection of the specimen is measured through the test by a deflection measuring devise fixed under the sample with direct contact with the specimen.

By this process, two sets of results were obtained for failure. One with consecutive strikes and the second with one strike. After saving the impact force wave of testing in the computer. The area under the impact force curve is integrated , multiplied by the value of force calibration and multiplied again by the impact velocity, yielding the absorbed energy.

4- Results and Discussion

4-1 Definition of Failure and Failure Energy Calculation

Sample failure is determined by examining the impacted sample. This involved visual and manual inspection of the failed area. Thus, cracks and delamination must take place between the upper and lower surfaces of the plate for it to be considered as failed sample.

The failure energy is calculated by multiplying the impact velocity with the area under the force-time curve. On the other hand, the total impact energy is calculated as the kinetic energy of the impacting steel ball.

4-2 The Effect of Curvature on Failure Energy

To study the effect of curvature on failure energy, the full set of experimental results presented in table (3) is examined. The relationship between samples radius, total and absorbed energy is shown in figure (4).

Table (3) Details of experimental test

Angle	Number of layer	Radius (cm)	High (cm)	Max. defl. (mm)	Max. force (N)	Total energy (J)	Abso. energy (J)	Abso. energy %
0°/90° W	10	12	425	30	2747.45	116.739	108.97	93.34
		20	400	27	2703.48	109.872	102.33	93.13
		30	375	24.4	2610.30	103.005	98.28	95.41
		45	350	23.6	2536.89	96.138	87.05	90.54
		flat	325	22	1947.77	89.271	57.24	64.11
0° U	10	12	350	29	3004.53	96.138	90.16	93.78
		20	325	26.2	2321.52	89.271	73.47	82.29
		30	300	23.6	2110.77	82.404	67.10	81.42
		45	275	22	1994.33	75.537	54.98	72.78
		flat	250	21	1869.01	68.67	47.226	68.77
0°/90° W	5	12	225	33	1468.82	61.803	51.628	83.53
		20	200	28	2012.51	54.936	47.361	86.21
		30	175	26	1858.74	48.069	39.573	82.32
		45	160	25	1507.55	43.948	34.562	78.64
		Flat	140	23	847.42	38.45	16.360	42.54
0° U	5	12	250	34	1831.25	68.670	61.114	88.99
		20	225	30	2172.11	61.803	54.866	88.77
		30	200	27	1708.95	54.936	45.891	83.53
		45	175	25	1466.25	48.069	38.739	80.59
		flat	150	21.5	950.67	41.202	21.939	53.24

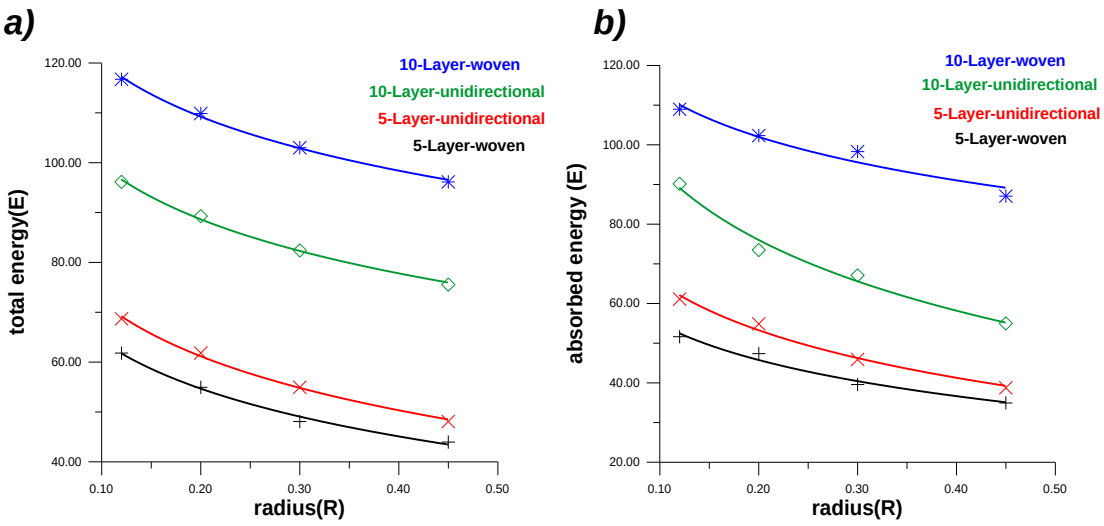

Figure (4) Relation between radius of with a- total energy b- absorbed energy

The energy required to fail samples are decreased for all cases with the increase in radius (i.e. decreased curvature). This is due to the decreased samples stiffness with increased curvature. Also, in all cases the ten layers woven samples absorbed more energy than the ten layers unidirectional samples.The opposite is observed for the five layer samples. In this case, the unidirectional plates are superior to the woven plates requiring more energy for failure.

The reasons for this contrast in the results can be attributed to the following:

1- The ten layers woven samples are more flexible than the unidirectional samples, thus absorbing more energy. Also the energy required to cause interlaminar delamination in the ten layers woven samples is larger than the energy required to delaminate fibers in the unidirectional samples.

2- The five layers unidirectional samples are more flexible than the woven samples and thus absorbing more energy. Also, the energy required to rupture fibers and cause delamination of fibers exceed that required for interlaminar delamination of the woven samples.

The absorbed energy values listed in table (3) compares well with reported values [**9**] except for the flat sample. The reported [**9**] conclusion of matrix crack and delamination accompanied by fiber cracks taking place when the absorbed energy exceed 75% of the total energy is validated. As can be seen in table (3), the absorbed energy in all tests, except for flat plate test, exceeds 75%.

4-3 The Effect of Number of layers on Failure Energy

To examine the effect of the number of layers on the energy required to fail the specimens of curved plates, samples of the tests are considered. Figure (5) shows the effect of change of the number of layers for four sets of (0° U) tests.

The failure (absorbed) energy calculated by integrating the area under the force-time diagram and multiplied by the impact velocity is shown in table (4).

Also, the total impact energy is calculated as the total kinetic energy of the impacting steel ball is presented in table (4).

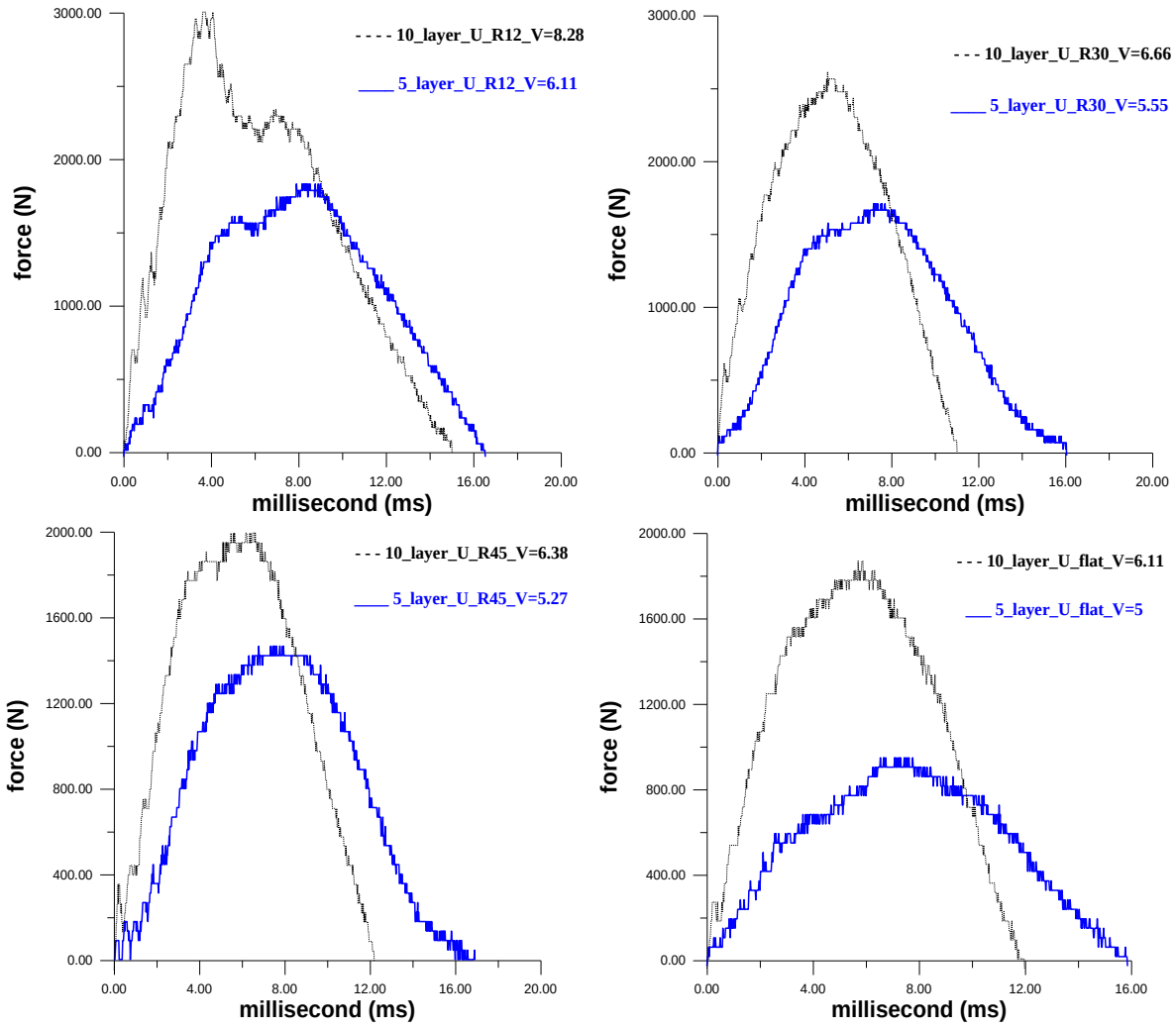

Figure (5) Effect of number of layers for unidirectional (0° U) at different radii

It is clear that for all tested curvature of composite plates, the failure energy has increased with the increase in the number of layers. This is obvious as larger thickness requires more energy to provide for matrix cracking and delamination between fibers and matrix as well as for fiber rupture.

Table (4) Total and absorbed energy in unidirectional samples

Number of layer	Radius (cm)	Total energy (J)	Abso. energy (J)	Number of layer	Radius (cm)	Total energy (J)	Abso. energy (J)
10	12	96.138	90.16	5	12	68.670	61.114
	30	82.404	67.10		30	54.936	45.891
	45	75.537	54.98		45	48.069	38.739
	flat	68.67	47.226		flat	41.202	21.939

Figure (6) shows the effect of change of the number of layers for four sets of (0°/90° W) tests. It can be seen that similar behavior to that of the (0° U) samples is observed. Table (5) shows the set of results for the energy requirements for the woven samples.

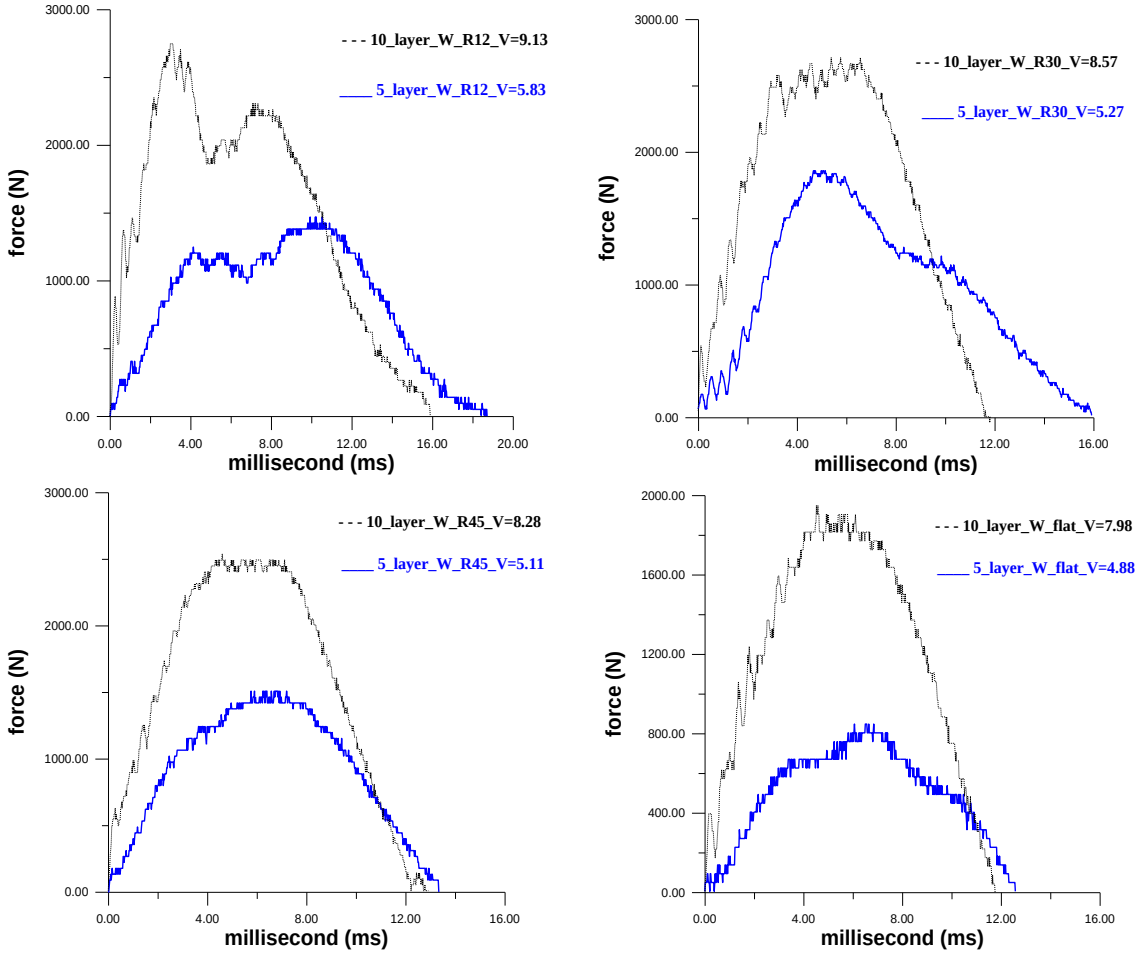

Figure (6) Effect of number of layers for woven (0°/90° W) at different radii

Table (5) Total and absorbed energy in woven samples

Number of layer	Radius (cm)	Total energy (J)	Abso. energy (J)	Number of layer	Radius (cm)	Total energy (J)	Abso. energy (J)
10	12	116.739	108.97	5	12	61.803	51.628
	30	103.005	98.28		30	48.069	39.573
	45	96.138	87.05		45	43.948	34.562
	flat	89.271	57.24		flat	38.45	16.360

A comparison of the total and absorbed energy listed in tables (4) and (5) show that the ten layers woven (0°/90° W) samples required more failure energy than the unidirectional (0° U) samples. The opposite is true for the five layers specimens. The reason for this is explained in the previous section.

4-4 The Effect of Lamination Angle on failure Energy

Two sets of eight results are chosen to illustrate the effect of lamination angle on failure energy. Figure (7) shows the force-time diagrams for the ten layers tests. The failure energy is calculated from these diagrams and listed in table (6).

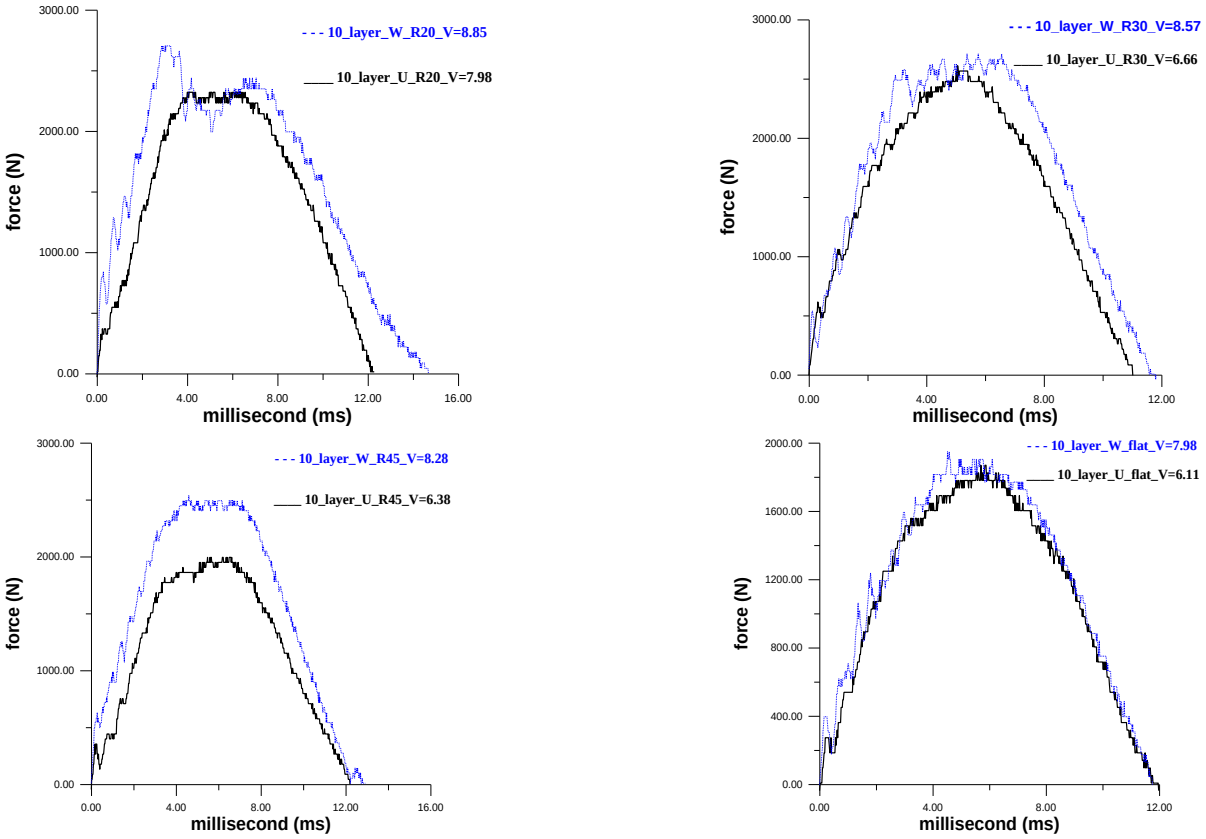

Figure (7) Effect of lamination angle of ten layers

Table (6) Total and absorbed energy in ten layers

Angle	Radius (cm)	Total energy (J)	Abso. energy (J)	Angle	Radius (cm)	Total energy (J)	Abso. energy (J)
0°/90° W	20	109.872	102.33	0° U	20	89.271	73.47
	30	103.005	98.28		30	82.404	67.10
	45	96.138	87.05		45	75.537	54.98
	flat	89.271	57.24		flat	68.67	47.226

It is clear that the energy required to fail the unidirectional samples are less than that required to fail the woven samples in all cases. Thus the woven type is superior to the unidirectional type.

The force-time diagrams for eight tests of the five layers samples are shown in figure (8) and the calculated energy results are shown in table (7).

In contrast with the results for the ten layers tests, the unidirectional samples absorbed more energy than the woven samples.

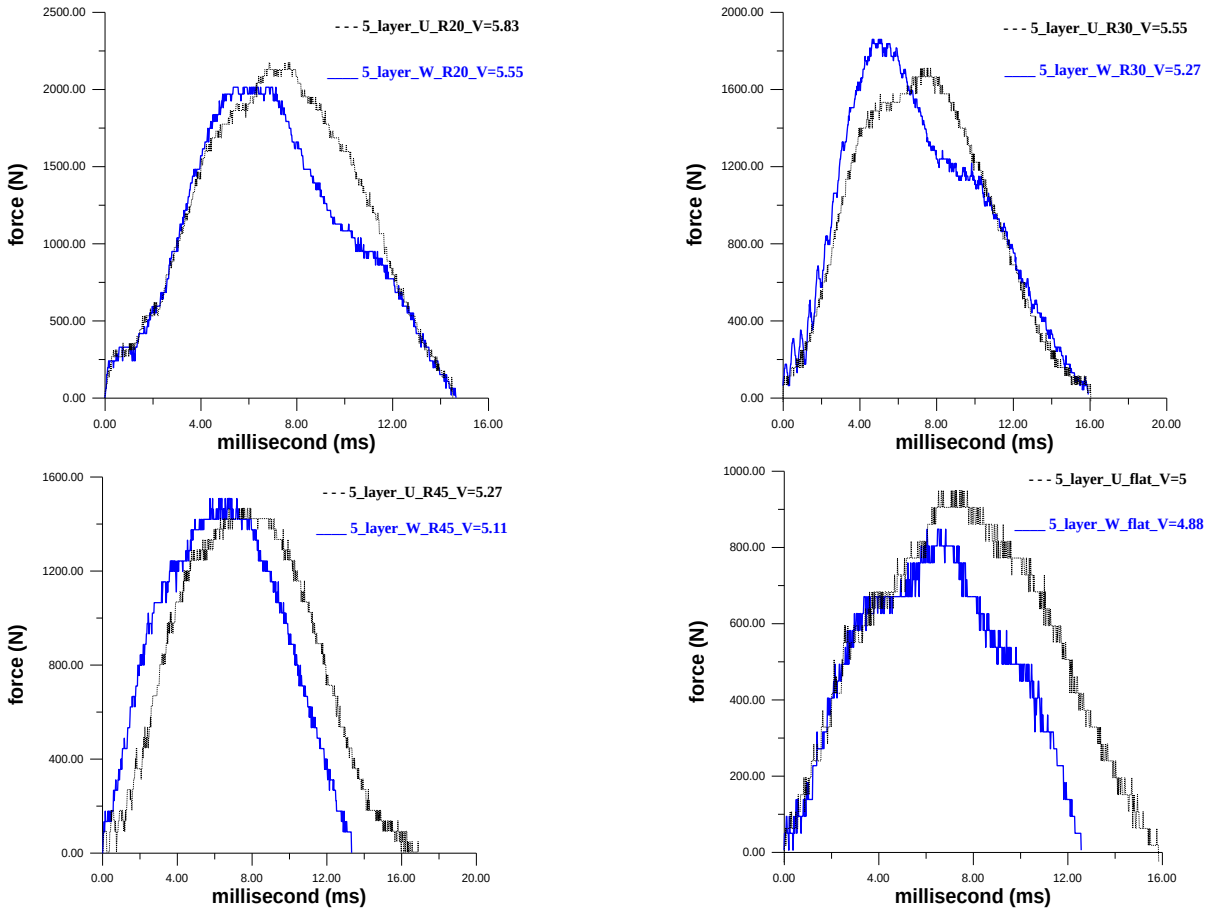

Figure (8) Effect of lamination angle of five layers

Table (7) Total and absorbed energy in Five layers

Angle	Radius (cm)	Total energy (J)	Abso. energy (J)	Angle	Radius (cm)	Total energy (J)	Abso. energy (J)
0°/90° W	20	54.936	47.361	0° U	20	61.803	54.866
	30	48.069	39.573		30	54.936	45.891
	45	43.948	34.562		45	48.069	38.739
	flat	38.45	16.360		flat	41.202	21.939

4-5 The Behavior of Woven and Unidirectional Specimens Under Multi Strike to Reach Failure

Multi strike tests are carried out by impacting the same specimen at different heights. Starting from a height of (0.5 m) for the five layers for both types of composite to a failure height in steps of (0.25 m). Then a height of (1.25 m) for the ten layers composite in steps of (0.25 m). The absorbed energy is calculated for each impact height by multiplying the impact velocity by the area under the force-time curve.

The calculated results for the woven specimens are shown in figure (9) and for the unidirectional samples in figure (10).

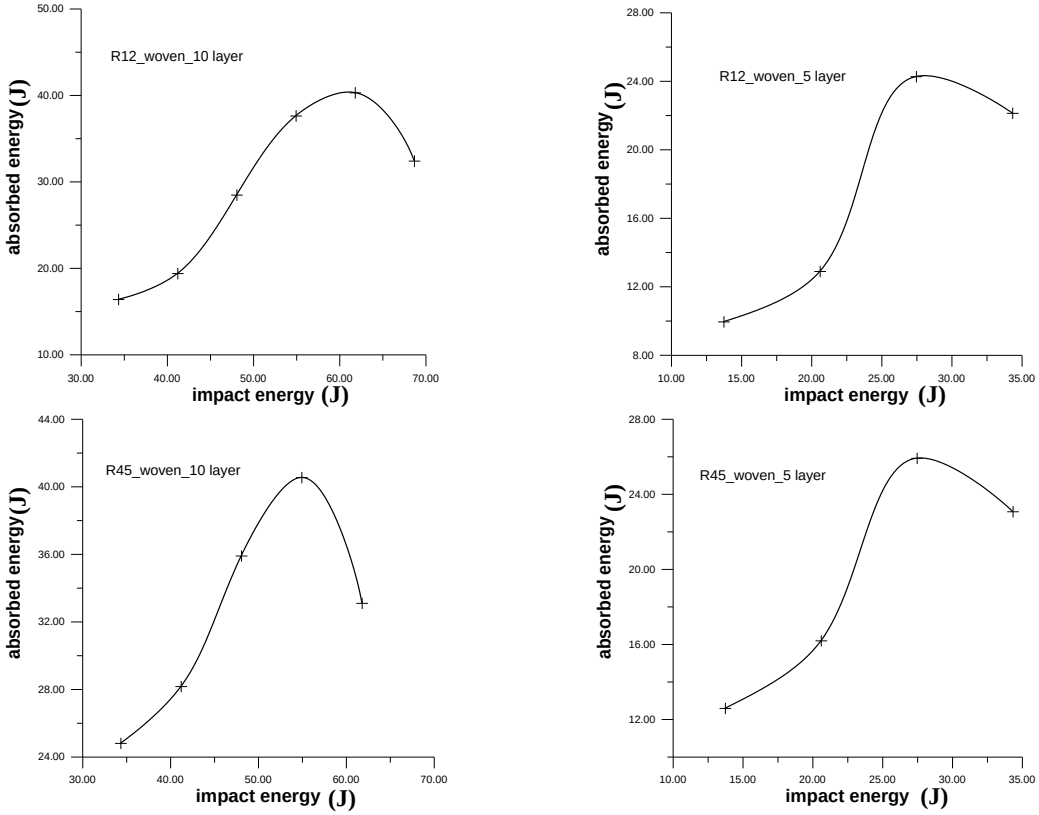

Figure (9) Behavior of woven sample consists of ten and five layers

These two sets of results show different energy absorbtion characteristics for the two types of composite. The woven specimens absorbed more and more energy, reaching a maximum level, then absorbing less energy up to failure. This behavior is most likely due to matrix cracking and interlaminar delamination occurring at the same time and absorbing increasing energy with increased impact energy. At the final stages of repeated impact, the interlaminar delamination is completed and only fiber rupture require less absorbed energy.

The ten and five layers specimen gave almost similar behavior with the ten layers specimens requiring obviously higher energy.

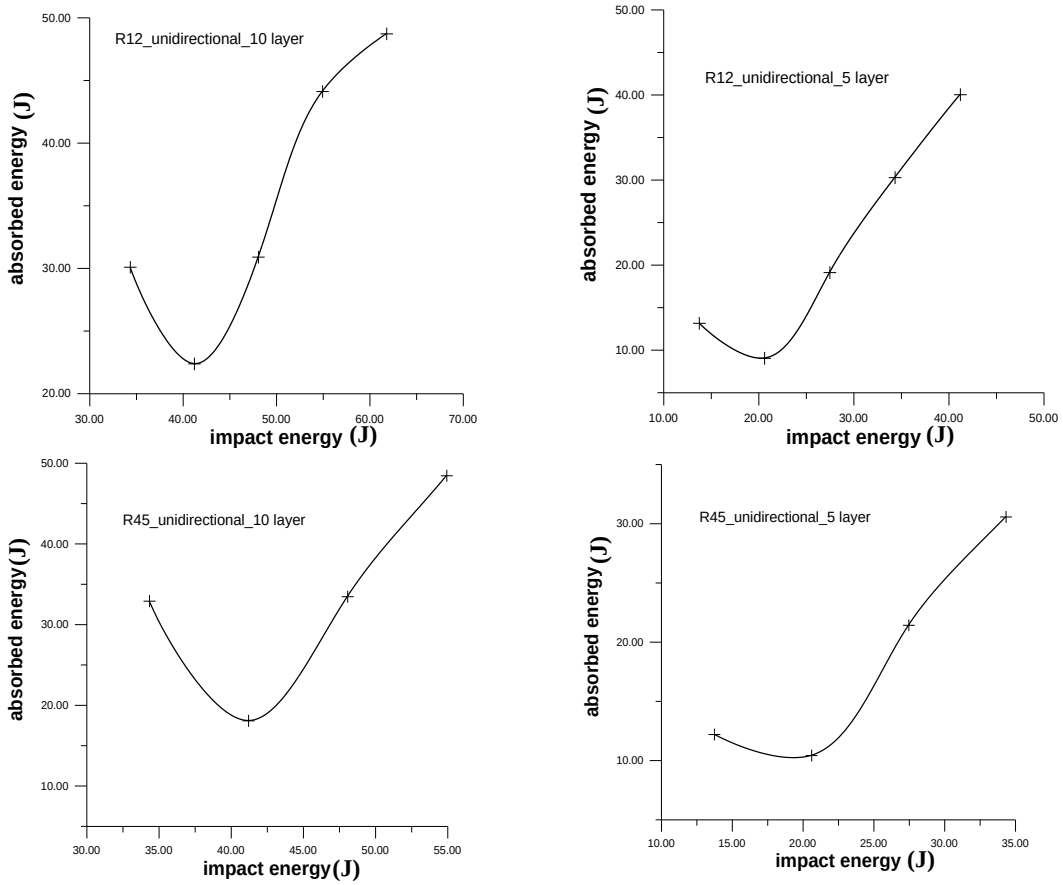

Figure (10) Behavior of unidirectional sample consists of ten and five layers

The unidirectional samples results in figure (10) showed a complete different pattern of energy absorbtion. This energy decreases initially, then increases continuously until failure. This behavior is due to initial delamination taking place between fibers which require little energy. Then a continuous process of fiber cracking and delamination requiring more and more energy till failure.

Also, the ten and five layers unidirectional specimen exhibit similar behavior as they both follow the same energy absorbtion characteristics.

A final remark is that similar energy absorbtion percentages of the energy associated with multi-strike tests as those in failure energy tests. For the ten layers woven samples, the failure energy in multi-strike tests is 50-60% of the failure energy in one strike. This percentage is 60-70% for the unidirectional samples. Nearly the same energy percentages applied for the five layers samples.

4-6 Form and Spread of Cracks in Woven and Unidirectional samples

In the ten layer unidirectional, thicker and thus less flexible laminates matrix cracks developed on the impacted face. These cracks are the result of high contact stresses induced beneath the impactor surface. They propagate vertically through the layers and initiate

delaminations when they reach lamina interfaces forming a "pine tree" pattern. Figure (11) shows the form of crack in a ten layer unidirectional sample on the top and lower surfaces.

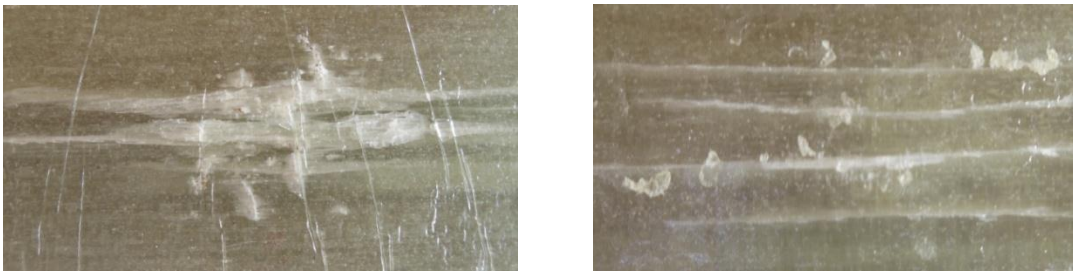

top surface ***lower surface***

Figure (11) Form of crack in ten layer unidirectional sample

In the five layer unidirectional, thinner and thus more flexible laminates matrix cracks developed on the lower face opposite the impacted face. These cracks result from bending and membrane stresses that induce large tensile strains on the backside of the laminate. These large tensile strains can result in transverse splitting of the fiber tows or even fiber fracture. The resulting cracks then propagate upwards and initiate delaminations at lamina interfaces forming a "reverse pine tree" pattern. Figure (12) shows the form of crack in a five layer unidirectional sample from the top and lower surfaces.

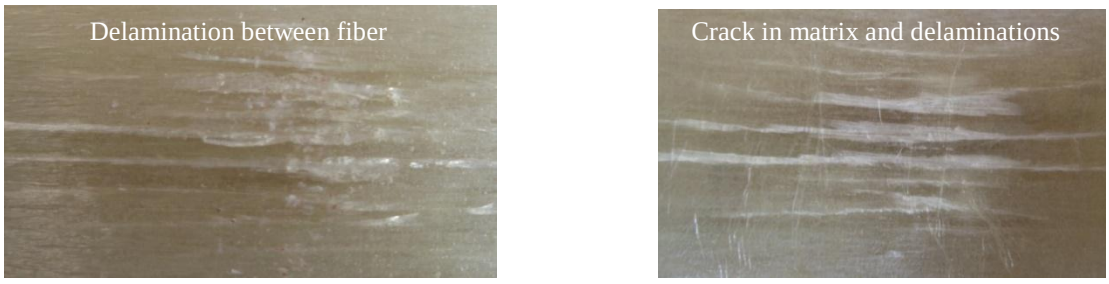

top surface ***lower surface***

Figure (12) Form of crack in five layer unidirectional sample

Due to the stacking sequence (0° U), the principal failure mechanism is matrix rupture, slightly reducing the global stiffness of the structure. Therefore, there is no abrupt drop of the impact force value after the progressive damage process initiation. Figure (13-a) shows some fiber fails damage more distributed at the matrix which is represented by cracks oriented along the fibers. Besides, it was observed that some fibers fail at the same or opposite side of impact of the specimens. This observation can explain why these specimens absorbed near 75% of the impact energy, where the failure mechanisms of fibers release more energy than failure mechanisms of the matrix. This behavior is similar to that reached by V. Tita, et al [**9**] as shown in figure (13-b).

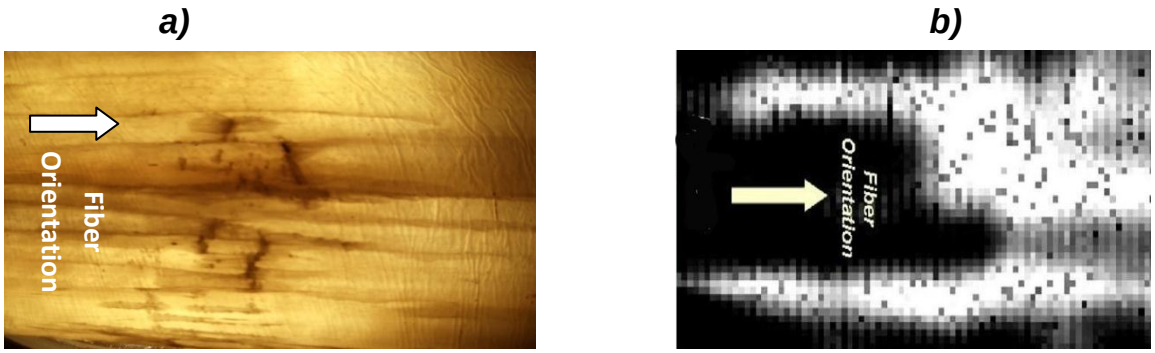

Figure (13) Form of crack in unidirectional sample with a) image under high light b) C-scan image [10]

In the woven samples, almost no difference is observed between the form of cracks in the five and ten layer samples. Starting from the top surface, large delamination area is formed and then delamination is spread between the layers. This create cracks in fibers along the width of the sample. Figure (14) shows the form of crack in woven sample in the top and lower surface.

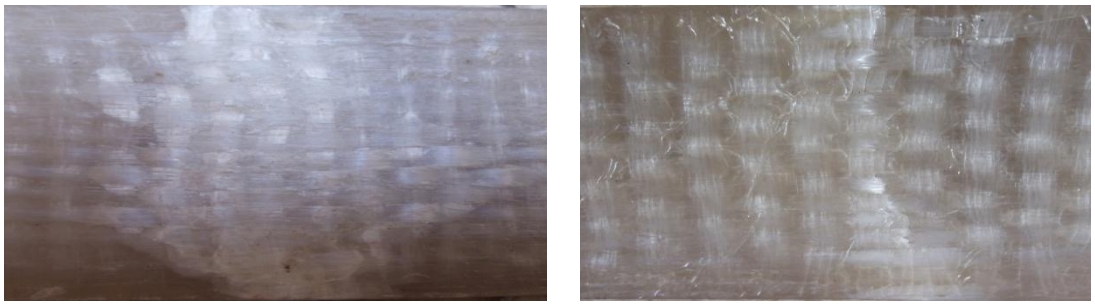

top surface ***lower surface***

Figure (14) Form of crack in woven sample

Due to the stacking sequence (0°/90° W), the main failure mechanisms are the matrix rupture and delamination, reducing the global stiffness of the structure. There are ‘‘peanut shapes’’, which represent delaminations, at both directions (0° and 90°). Figure (15-a) show damage under high light. This behavior is the same as that observed by V. Tita, et al [**9**] for epoxy resin reinforce by carbon fiber as shown in figure (15-b).

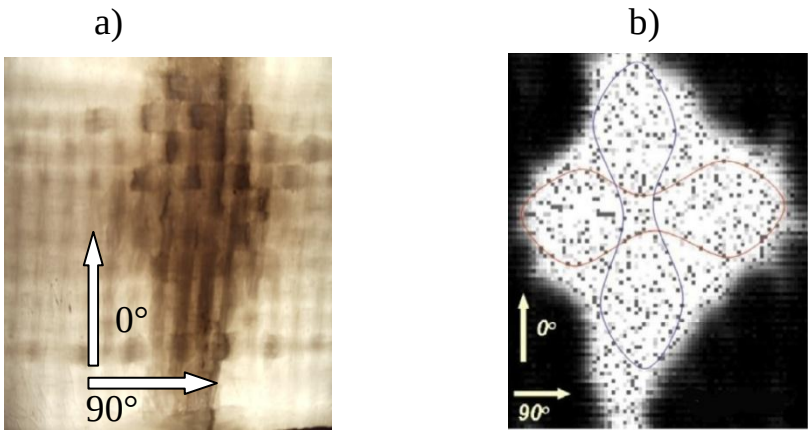

Figure (15) Form of crack in woven sample with a) image under high light b) C-scan image [10]

Conclusions

The following remarks can be concluded:

1- With increased curvatures higher force and failure energy was required at all tested velocities.
2- Increase in both, impact force and energy is required to fail samples with increased number of layers at all tested velocities.
3- In ten layers, the energy required to fail the woven samples is higher than the energy required to fail similar unidirectional samples.
4- In five layers, the energy required to fail the unidirectional samples is higher than the energy required to fail similar woven samples.
5- In five layers unidirectional matrix, cracks occur on the face opposite the impact face. The resulting cracks then propagate upwards and initiate delaminations at lamina interfaces forming a “reverse pine tree” pattern.
6- In ten layers unidirectional matrix, cracks occur on the impacted face. They propagate vertically through the layers and initiate delaminations when they reach lamina interfaces forming a “pine tree” pattern.

References

[1]Zaid R.M. Al.Ani, "**Flexural Analysis of Composite Laminated Simply Supported Rectangular Beam**". M.Sc. Thesis, Al-Mustansiriya university, February (2006).

[2]L.S. Sutherland , C. Guedes Soares, "**Impact Tests on Woven-Roving E-glass/Polyester Laminates**", Composites Science and Technology, Vol.59, pp.1553-1567,(1999).

[3]R. Tiberkak, M. Bachene, S. Rechak, B. Necib, "**Damage Prediction in Composite Plates Subjected to Low Velocity Impact**", Composite Structures, Vol.83, pp.73-82,(2008).

[4]Kurt Henkhaus, "**Overview of Research on Composite Material Impact Behavior**", University of Kansas.

[5]A.F. Johnson, A.K. Pickett, P. Rozycki, "**Computational Methods for Predicting Impact Damage in Composite Structures**", Composites Science and Technology, Vol.61, pp.2183–2192, (2001).

[6]Tien-Wei Shyr, Yu-Hao Pan, "**Impact Resistance and Damage Characteristics of Composite Laminates**", Composite Structures, Vol.62, pp.193–203,(2003).

[7]L.S. Sutherland, C. Guedes Soares, "**Impact on Low Fibre-volume, Glass/Polyester Rectangular Plates**", Composite Structures, Vol.68, pp.13–22, (2005).

[8]R. Hosseinzadeh, M.M. Shokrieh, L. Lessard, "**Damage Behavior of Fiber Reinforced Composite Plates Subjected to Drop Weight Impacts**", Composites Science and Technology, Vol.66, pp.61–68,(2006).

[9]V. Tita, J. de Carvalho, D. Vandepitte, "**Failure Analysis of Low Velocity Impact on Thin Composite Laminates: Experimental and Numerical Approaches**", Composite Structures, Vol.83, pp.413–428,(2008).

[10]G.A.O. Davies, X. Zhang, "**Impact Damage Prediction in Carbon Composite Structures**", Int. J. Impact Engng Vol.16, No. 1, pp.149-170,(1995).

[11]Shiuh-Chuan Her, Yu-Cheng Liang, "**The Finite Element Analysis of Composite Laminates and Shell Structures Subjected to Low Velocity Impact**", Composite Structures, Vol.66, pp.277–285,(2004).

[12]S. Ganapathy, K.P. Rao, "**Failure Analysis of Laminated Composite Cylindrical/Spherical Shell Panels Subjected to Low-Velocity Impact**", Computers and Structures, Vol.68, pp.627-641, (1998).

[13]S.M.R. Khalili, M. Soroush, A. Davar, O. Rahmani, "**Finite Element Modeling of Low-Velocity Impact on Laminated Composite Plates and Cylindrical Shells**", Composite Structures, Vol.93, pp1363–1375,(2011).

[14]K.S. Krishnamurthy, P. Mahajan, R.K. Mittal, "**Impact Response and Damage in Laminated Composite Cylindrical Shells**", Composite Structures, Vol.59, pp.15–36,(2003).

[15]S. Jo Kim, N. Seo Goo, T. Won Kim, "**The Effect of Curvature on the Dynamic Response and Impact-Induced Damage in Composite Laminates",** Composites Science and Technology, Vol.51, pp.763-773**,** (1997).

[16]S. KUMAR, "**Analysis of Impact Response and Damage in Laminated Composite Shell Involving Large Deformation and Material Degradation**", J. Mechanics Of Materials And Structures, Vol.3, No.9,Nov.(2008).

[17]J.-M. Berthelot," **Mechanical Behaviour of Composite Materials and Structures**", Institute for Advanced Materials and Mechanics, Le Mans, France, (1999).

[18]G., Lubin, "**Handbook of Composites**", Van Nostrand Reinhold, USA, (1982).